

**PASSIVATION OF DEFECT STATES IN Si AND Si/SiO<sub>2</sub> INTERFACE STATES BY  
CYANIDE TREATMENT: IMPROVEMENT OF CHARACTERISTICS OF  
PIN-JUNCTION AMORPHOUS Si AND CRYSTALLINE Si-BASED  
METAL-OXIDE-SEMICONDUCTOR JUNCTION SOLAR CELLS \***

**N. Fujiwara, T. Fujinaga, D. Niinobe, O. Maida, M. Takahashi, H. Kobayashi**

*Institute of Scientific and Industrial Research, Osaka University*

*and*

*CREST, Japan Science and Technology Corporation,*

*8-1 Mihogaoka, Ibaraki, Osaka 567-0047, Japan*

Received 4 December 2002, in final form 29 April 2003, accepted 29 April 2003

Defect states in Si can be passivated by cyanide treatment which simply involves immersion of Si materials in KCN solutions, followed by rinse. When the cyanide treatment is applied to pin-junction amorphous Si (a-Si) solar cells, the initial conversion efficiency increases. When the crown-ether cyanide treatment using a KCN solution of xylene containing 18-crown-6 is performed on i-a-Si films, decreases in the photo- and dark current densities with the irradiation time are prevented. The cyanide treatment can also passivate interface states present at Si/SiO<sub>2</sub> interfaces, leading to an increase in the conversion efficiency of (ITO/SiO<sub>2</sub>/Si(100)) solar cells. Si-CN bonds formed by the reaction of defect states with cyanide ions have a high bond energy of about 4.5 eV and hence heat treatment at 800 °C does not rupture the bonds, making thermal stability of the cyanide treatment. When the cyanide treatment is applied to ultrathin SiO<sub>2</sub>/Si structure, the leakage current density is markedly decreased.

PACS: 85.60.Dw, 81.60.Cp, 73.20.Hb, 85.40.Hp

## **1 Introduction**

Defect states in the band-gap seriously degrade Si solar cell characteristics. In the case of amorphous Si (a-Si), an intrinsic layer (i-layer) with good characteristics has a defect density of the order of  $10^{21} \text{ m}^{-3}$ , but it increases to the order of  $10^{23} \text{ m}^{-3}$  with prolonged irradiation [1]. In the absence of defect states, almost a uniform electrical field is induced in the i-layer by charges in the n- and p-layers as shown in Fig. 1a. However, light irradiation generates defect states in the band-gap of a-Si. Photo-generated electrons and holes are trapped at the defect states near the n/i- and p/i-interfaces, respectively, and consequently the potential gradient in these regions becomes steep (Fig. 1b). However, the band in the middle of the i-layer becomes flat, and photo-generated electrons and holes recombine at the defect states, resulting in a decrease in the energy conversion efficiency. Due to the formation of defect states, photo- and dark conductivities of a-Si films greatly decrease with the irradiation time, as was observed by Staebler and Wronski in 1977 for

\*Presented at Workshop on Solid State Surfaces and Interfaces III, Smolenice, Slovakia, November 19 – 21, 2002.

the first time [2]. Since then, extensive studies have been performed to prevent the light-induced degradation, but no method of complete prevention has been developed so far. Many models for the Staebler-Wronski effect including the weak bond model [3, 4], bistable dangling bond model [5], floating-bond model [6], charge-capturing model [7], impurity-related model [8], structural change model [9], etc. are proposed but its detailed mechanism still remains unresolved. Metal-oxide-semiconductor (MOS) structure is very important not only for solar cells but also for the application to LSI and thin film transistor (TFT). In the case of MOS-type solar cells, the thickness of a silicon dioxide ( $\text{SiO}_2$ ) layer is less than 1.5 nm to allow a photocurrent to tunnel [10]. In the case of MOS diodes in LSI, miniaturization requires the usage of ultrathin  $\text{SiO}_2$  layers. In fact, the Semiconductor Roadmap predicts that the equivalent oxide thickness for the devices with a 80 nm design rule produced in 2005 decreases to 0.8 up to 1.3 nm [11]. For such ultrathin  $\text{SiO}_2$  layers, Si/ $\text{SiO}_2$  interfaces, especially interface states in the Si band-gap, play an important role in the determination of electrical characteristics. The Si/ $\text{SiO}_2$  interface states are usually passivated by hydrogen treatment (i.e., heat treatment in hydrogen atmospheres at 250 to 450°C [12, 13], and the passivation is attributed to the formation of Si-H bonds from Si dangling bonds [14]. However, the Si-H bonds have a relatively low bond energy of 3.1 to 3.5 eV [15, 16], and thus heat treatment above 550 to 600°C ruptures the bonds [17], resulting in the regeneration of interface states. Moreover, irradiation forms atomic hydrogen in a  $\text{SiO}_2$  layer, and when it diffuses to the Si/ $\text{SiO}_2$  interface, it reacts with Si-H, resulting in the formation of Si dangling bond interface states [18, 19].

Metal-oxide-semiconductor (MOS) structure is very important not only for solar cells but also for the application to LSI and thin film transistor (TFT). In the case of MOS-type solar cells, the thickness of a silicon dioxide ( $\text{SiO}_2$ ) layer is less than 1.5 nm to allow a photocurrent to tunnel [10]. In the case of MOS diodes in LSI, miniaturization requires the usage of ultrathin  $\text{SiO}_2$  layers. In fact, the Semiconductor Roadmap predicts that the equivalent oxide thickness for the devices with a 80 nm design rule produced in 2005 decreases to 0.8 ~ 1.3nm [11]. For such ultrathin  $\text{SiO}_2$  layers, Si/ $\text{SiO}_2$  interfaces, especially interface states in the Si band-gap, play an important role in the determination of electrical characteristics. The Si/ $\text{SiO}_2$  interface states are usually passivated by hydrogen treatment (i.e., heat treatment in hydrogen atmospheres at 250 to 450°C [12, 13]), and the passivation is attributed to the formation of Si-H bonds from Si dangling bonds [14]. However, the Si-H bonds have a relatively low bond energy of 3.1 to 3.5 eV [15, 16], and thus heat treatment above 550 ~ 600°C ruptures the bonds [17], resulting in the regeneration of interface states. Moreover, irradiation forms atomic hydrogen in a  $\text{SiO}_2$  layer, and when it diffuses to the Si/ $\text{SiO}_2$  interface, it reacts with Si-H, resulting in the formation of Si dangling bond interface states [18, 19].

In the present study, a new method of passivating defect states in a-Si films and Si/ $\text{SiO}_2$  interface states has been developed. This method called "cyanide treatment" simply involves immersion of Si materials in cyanide solutions [20, 21, 22, 23]. Cyanide ions ( $\text{CN}^-$ ) react selectively with defect states, resulting in the formation of strong Si-CN bonds.

## 2 Experiments

The p - a - SiC/350nm i - a - Si/n-type micro-crystalline ( $\mu\text{c}$ ) Si (hereafter this structure is abbreviated as pin-a-Si) layers were deposited on transparent conductive oxide (TCO) by use of

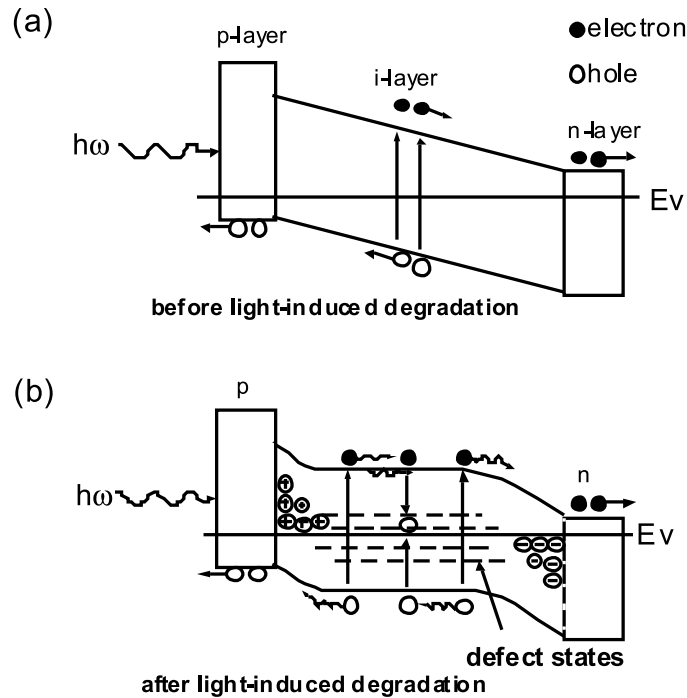


Fig. 1. Band diagrams of pin-junction a-Si solar cells: (a) before light-induced degradation; (b) after light-induced degradation

a plasma-enhanced chemical vapor deposition (PECVD) method. The 350 nm (i-a-Si/TCO) structure was also formed using PECVD. The cyanide treatment was performed using the following two methods. For the (pin-a-Si/TCO) structure, the specimens were simply immersed in 1 M or 0.1 M KCN aqueous solutions for 2 min, followed by the rinse in boiling water (aqueous cyanide treatment). This aqueous cyanide treatment was possible because unlike i-a-Si, the n-c-Si layer did not dissolve in the KCN aqueous solutions (i.e., strong alkaline solutions).

In the case of the i-a-Si/TCO structure, crown-ether cyanide treatment was performed by use of a KCN solution of xylene containing 18-crown-6. An 18-crown-6 molecule possesses a hole of 0.27 nm diameter and a potassium ion of 0.266 nm diameter just fits the hole. When the potassium ion enters the hole, it is strongly captured by six oxygen atoms pointing toward the hole. Therefore, inclusion of 18-crown-6 in the KCN solution completely prevents contamination by potassium ions [22]. This crown-ether cyanide treatment was also performed on the (pin-a-Si/TCO) structure. After the crown-ether cyanide treatment, the specimens were rinsed in succession with acetone, ethanol, and ultra-pure water at 25°C. Aluminum (Al) electrodes of 3.0 mm diameter were formed on the a-Si film for the current collection.

MOS structure was fabricated using phosphorus-doped n-type single crystalline Si (100) wafers of about 0.1 Ωm resistivity. After cleaning the wafers using the RCA method, an ul-

trathin SiO<sub>2</sub> layer of thickness less than 2.3 nm was formed by heat treatment at temperatures ranging between 450 and 650°C in wet-oxygen, and then crown-ether cyanide treatment or aqueous cyanide treatment was performed. 0.15 mm diameter Al electrodes were formed on the SiO<sub>2</sub> layer, resulting in the ⟨Al/ultrathin SiO<sub>2</sub>/Si(100)⟩ MOS structure. In the case of solar cell applications, mat-textured Si surfaces were produced by alkaline etching [24] and ultrathin SiO<sub>2</sub> layers were formed, followed by the deposition of indium tin oxide (ITO) films by a spray pyrolysis method [25].

### 3 Results and discussion

#### 3.1 Cyanide treatment of a-Si

Fig. 2 shows the photocurrent density vs. photovoltage ( $I_{ph} - V_{ph}$ ) curves for the ⟨Al/pin - a - Si/TCO⟩ solar cells before light-induced degradation. The  $I_{ph} - V_{ph}$  curves were measured under AM 1.5 1mW/mm<sup>2</sup> irradiation. With no treatment, the fill factor (FF) was relatively low (0.604) and the energy conversion efficiency ( $\eta$ ) was 6.4% (curve a). When the cyanide treatment using the 1 M (or 0.1 M) KCN aqueous solution was performed on the nip-a-Si/TCO structure (curve b for 0.1 M and curve c for 1 M), the FF and  $\eta$  were improved to 0.743 and 8.23%, respectively (or 0.667 and 7.44%, respectively). These improvements are attributable to the passivation of defect states present before irradiation by CN<sup>-</sup> ions. The greater improvement using the 1 M KCN solution than that using the 0.1 M solution shows that a high concentration of CN<sup>-</sup> ions are necessary to passivate the defect states in the i-a-Si layer probably because of the presence of the n -  $\mu$ c - Si overlayer which blocks the penetration of CN<sup>-</sup> ions, during the cyanide treatment. The crown-ether cyanide treatment could not improve the  $I_{ph} - V_{ph}$  characteristics reproducibly possibly because of a low concentration of CN<sup>-</sup> ions in the solution. It should be noted that in spite of the absence of ZnO and Ag electrodes for light trapping, the conversion efficiency of the a-Si solar cells with the cyanide treatment was considerably high.

Fig. 3 shows the  $I_{ph} - V_{ph}$  curves for the ⟨Al/pin - a - Si/TCO⟩ solar cells after 5 sun irradiation for 25 h in an open circuit condition. In the open circuit condition, all photo-generated electron-hole pairs recombine, leading to the enhancement of light-induced degradation.  $\eta$  and FF for the solar cells with no treatment (curve a), and 0.1 M (curve b) and 1 M (curve c) KCN treatments were 5.19% and 0.525, 5.43% and 0.547, and 6.30% and 0.623, respectively. The FF and for the solar cells with cyanide treatment were still higher than those for the cells with no treatment. This result indicates that Si-CN bonds formed by the cyanide treatment are not ruptured by irradiation. However, the solar cells with the cyanide treatment still showed light-induced degradation. This degradation is likely to be caused by the formation of defect states from defect precursor states.

The above results indicate that defect states present before light irradiation can be passivated by the cyanide treatment, resulting in the improvement in the initial conversion efficiency. However, defect precursor states cannot be eliminated by the cyanide treatment, probably because sufficiently high concentration of CN<sup>-</sup> ions do not penetrate near the p/i interface, and thus the defect formation occurs there by irradiation. It is expected that the enhancement of the migration of CN<sup>-</sup> ions in a-Si can passivate defect precursor states present near the p/i interface, resulting in the prevention of light-induced degradation.

Fig. 4 shows the photo- and dark current densities of the ⟨Al/350nm i - a - Si/TCO⟩

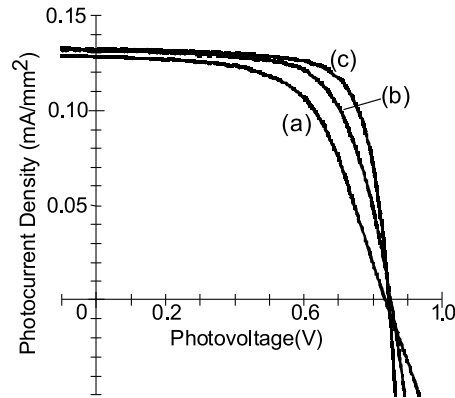


Fig. 2. The  $I_{ph} - V_{ph}$  curves for the a-Si solar cells with the  $\langle \text{Al/pin} - \text{a-Si/TCO} \rangle$  structure before light-induced degradation: (a) with no treatment; (b) with cyanide treatment using the 0.1 M KCN aqueous solution; (c) with cyanide treatment using the 1 M KCN aqueous solution

structure measured as a function of the 3 sun irradiation in an open-circuit condition. During the crown-ether cyanide treatment, a bias voltage of 8 V was applied to the TCO film with respect to the platinum (Pt) counter electrode for the enhancement of the inward migration of  $\text{CN}^-$  ions. The application of 8 V was possible because, unlike water, xylene did not decompose. For the application of a bias voltage during the crown-ether cyanide treatment, a-Si films had to be deposited on TCO, and consequently the current was measured between the front and back sides of the a-Si films, rather than by the gap-cell system usually employed for conductivity measurements. The photocurrent density was measured under AM 1.5  $1 \text{ mW/mm}^2$  irradiation. During the current measurements, a bias voltage of 0.2 V was applied to the Al electrode with respect to the TCO film. In the open-circuit condition, all photo-generated holes and electrons recombine, leading to the high defect formation rate. We observed that the rate of the decrease in the photocurrent density caused in the short-circuit condition was only about 1/5 of that in the open-circuit condition.

The photocurrent density of the specimens that did not receive crown-ether cyanide treatment markedly decreased with the irradiation time (curve a). The dark current density also decreased greatly (curve d). When the crown-ether cyanide treatment was performed under 8 V applied to the specimen with respect to the Pt counter electrode, photo- and dark current densities did not decrease at all (curves b and e). In this case, the photocurrent density increased with the irradiation time. With the crown-ether cyanide treatment in which no bias was applied to the specimen, the photo- and dark current densities still decreased with the irradiation time but their rates became much lower (curves c and f).

Considering that the capacitance of the Helmholtz layer (i.e., the electrical double layer at the solid/liquid interface) is in the range of  $0.2 \mu\text{F/mm}^2$  [26] — much larger than that of the i-a-Si film — most of the external bias is consumed across the i-a-Si film, inducing an electrical field in the film. When the positive bias voltage is applied to the specimen during the crown-ether cyanide treatment, the migration of  $\text{CN}^-$  ions into the i-a-Si film is enhanced by the electrical

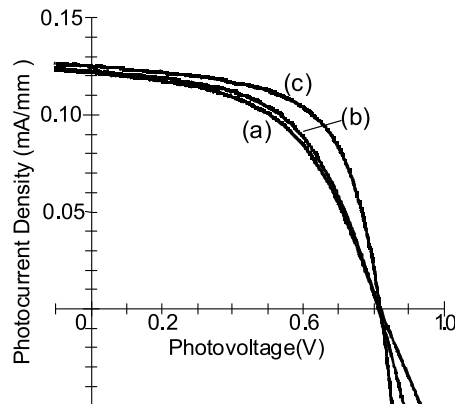


Fig. 3. The  $I_{ph} - V_{ph}$  curves for the a-Si solar cells with the  $\langle \text{Al/pin} - \text{a} - \text{Si/TCO} \rangle$  structure after light-induced degradation: (a) with no treatment; (b) with cyanide treatment using the 0.1 M KCN aqueous solution; (c) with cyanide treatment using the 1 M KCN aqueous solution.

field, and consequently defect and defect precursor states throughout the film are eliminated. Without the application of a positive bias voltage during the crown-ether cyanide treatment,  $\text{CN}^-$  ions cannot penetrate deeply into the film and consequently photo-degradation is only partially prevented.

The photo-degradation of the i-a-Si layer is prevented by the crown-ether cyanide treatment performed before irradiation, i.e., before photo-generation of defect states. From this result, the mechanism of defect elimination can be deduced as follows: Without crown-ether cyanide treatment, defect precursor states are present before irradiation (Fig. 5a) and they are converted to defect states with irradiation (Fig. 5b). With crown-ether cyanide treatment, though, the defect precursor states as well as defect states are eliminated by a reaction with  $\text{CN}^-$  ions to form strong Si-CN bonds (Fig. 5c). As a result, defect states do not occur with irradiation (Fig. 5d). The experimental results support models for the Staebler-Wronski effect in which defect precursor states present before irradiation are converted to defect states by irradiation. The experimental results favor models in which defect and defect precursor states possess similar structures as in the bistable dangling bond model [5] (defect precursor states:  $\text{sp}^3$ -like Si dangling bonds with negative-U, defect states:  $\text{p}^2$ -like Si dangling bonds with positive-U).

The increase in the photocurrent density with irradiation time after the crown-ether cyanide treatment (Fig. 4b) probably results from the enhancement by incident light of the migration and/or reaction of unreacted  $\text{CN}^-$  ions in the i-a-Si:H film with defect states.

### 3.2 Cyanide treatment of Si/SiO<sub>2</sub> structure

Fig. 6 shows the conductance-voltage ( $G - V$ ) curves for the  $\langle \text{Al/} 2\text{nm SiO}_2/\text{Si}(100) \rangle$  MOS diodes. The background due to the leakage current was estimated from the derivative of the current density with respect to the bias, and subtracted from the observed curves. Therefore, the conductance shown in Fig. 6 was approximately in proportion to the interface state density [27].

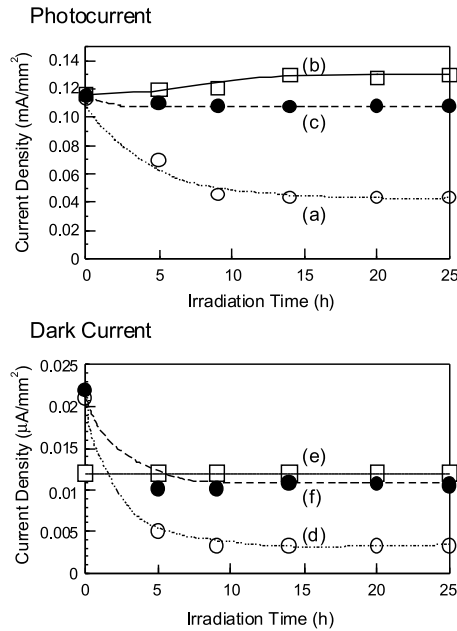


Fig. 4. Photo- (a to c) and dark (d to f) current densities of the 350 nm i-a-Si films with the  $\langle \text{Al/i-a-Si/TCO} \rangle$  structure as a function of the 3 sun irradiation time: (a) and (d) with no treatment; (b) and (e) with crown-ether cyanide treatment under 8 V; (c) and (f) with crown-ether cyanide treatment under no bias.

With no treatment (curve a), the conductance was high, indicating the presence of high density interface states. The conductance was decreased to about 1/10 by crown-ether cyanide treatment (curve b), showing that most of the interface states were passivated. When the SiO<sub>2</sub>/Si structure with the crown-ether cyanide treatment was heated at 800°C in nitrogen, the conductance did not increase at all. This result indicates that Si-CN bonds formed by the cyanide treatment are not ruptured at 800°C. This thermal stability is an important advantage of the cyanide treatment over the hydrogen treatment in which Si-H bonds are broken at 550 ~ 600°C [17]. We have found from theoretical calculations using a density functional theory method that Si-CN bonds possess a bond energy of about 4.5 eV, i.e., more than 1 eV higher than the Si-H bond energy [15, 16]. The thermal stability of the cyanide treatment is attributable to the high Si-CN bond energy.

Fig. 7 shows the  $I_{ph} - V_{ph}$  curves for the  $\langle \text{ITO/SiO}_2/\text{Si}(100) \rangle$  MOS solar cells. The SiO<sub>2</sub> layer was formed at 450° C in wet-oxygen and its thickness was less than 1.5 nm to allow a photocurrent easily to tunnel. The photocurrent density was high (i.e., about 0.4 mA/mm<sup>2</sup> under AM 1.51mW/m<sup>2</sup> irradiation), because of the formation of a mat-textured Si surface and the anti-reflection coating effect of the ITO film. However, the production of the mat-textured surface resulted in the formation of high-density interface states, leading to a low photovoltage (curve a). When the cyanide treatment was performed on the mat-textured Si surface, the open-circuit photovoltage ( $V_{OC}$ ) increased by 80 mV (curve b).  $V_{OC}$  is determined by the ratio between the photocurrent density,  $J_{ph}$ , and the reverse bias dark saturation current density,  $J_{dark}^0$  [28]:

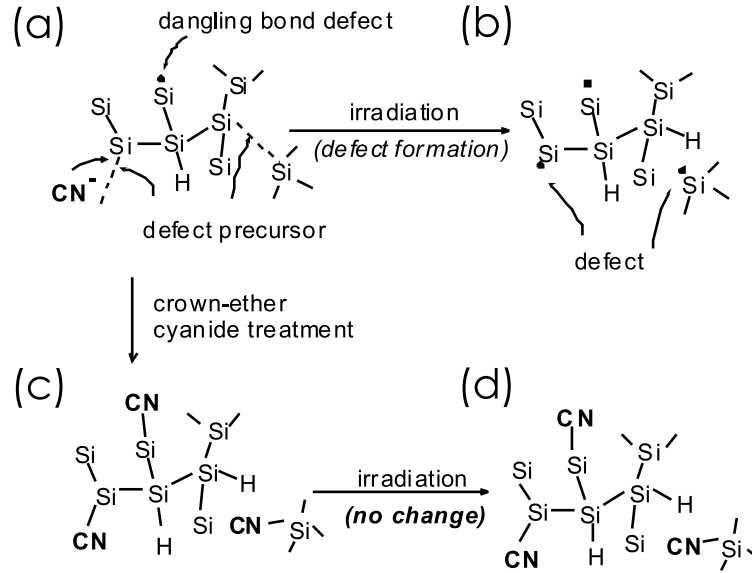


Fig. 5. Schematic diagrams of i-a-Si films: (a) before irradiation; (b) after irradiation on untreated films; (c) with cyanide treatment before photo-degradation; (d) after irradiation on films with cyanide treatment.

$$V_{OC} = \frac{nkT}{e} \ln \left( \frac{J_{ph}}{J_{dark}^0} + 1 \right), \quad (1)$$

where  $n$  is the ideality factor. Eqn.(1) shows that for an increase in  $V_{OC}$  by 80 mV,  $J_{dark}^0$  should be reduced to about 1/20 (or about 1/5), assuming the ideality factor is unity (or 2). This vast decrease in  $J_{dark}^0$  results from the elimination of interface states, leading to i) a decrease in the interface recombination current density and ii) an increase in the Si band-bending due to the unpinning of the interfacial Fermi level.

For the MOS-type solar cells, the  $\text{SiO}_2$  layers are necessary to be thin (less than 1.5 nm) for a photocurrent to tunnel smoothly. For  $G - V$  measurements, on the other hand, the  $\text{SiO}_2$  layers should be sufficiently thick (thicker than 2 nm) to decrease the background due to the leakage current. Therefore, it is impossible to perform the measurements of solar cell characteristics and the  $G - V$  characteristics using the same specimens. Although the same MOS diodes cannot be employed for the  $G - V$  and solar cell characteristics measurements for the above reason, we have obtained the results that the solar cell characteristics are improved by the cyanide treatment, and that interface states are eliminated by the same treatment. Therefore, it is highly probable that the improvement of the solar cell characteristics results from the elimination of interface states. The conversion efficiency of the  $\langle \text{ITO}/\text{SiO}_2/\text{Si}(100) \rangle$  MOS solar cells with the cyanide treatment was found to be constant during the AM 1.5  $1\text{mW}/\text{mm}^2$  irradiation period for more than 1,000 h. This result clearly shows that Si-CN bonds are not ruptured upon irradiation.

Fig. 8 shows the current-voltage ( $I - V$ ) curves of the  $\langle \text{Al}/2.3\text{nm SiO}_2/\text{Si}(100) \rangle$  MOS diodes with the  $\text{SiO}_2$  layer formed at  $650^\circ\text{C}$  in wet-oxygen, measured in the dark. With no

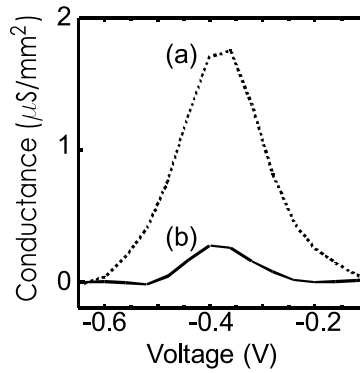


Fig. 6. The  $G - V$  curves for the  $\langle \text{Al}/2\text{nmSiO}_2/\text{Si}(100) \rangle$  MOS diodes after the subtraction of the background: (a) with no treatment; (b) with crown-ether cyanide treatment.

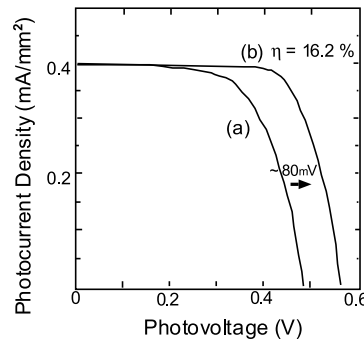


Fig. 7. The  $I_{ph} - V_{ph}$  curves for the  $\langle \text{ITO}/\text{SiO}_2/\text{Si}(100) \rangle$  MOS solar cells: (a) with no treatment; (b) with cyanide treatment.

treatment, the leakage current density was relatively high (curve a) possibly because of the low oxidation temperature [29]. With the crown-ether cyanide treatment, the leakage current densities in the positive (i.e., forward) and negative (reverse) bias regions were decreased to (1/8 and (1/3, respectively. This decrease in the dark current density is attributable to the elimination of interface states.

In the accumulation condition, electrons in the Si bulk transfer to the Si/SiO<sub>2</sub> interface with no energy barrier and then they are trapped at the interface states, followed by tunneling to the metal. Since the transition from the Si conduction band to interface states requires no activation energy, interface states with energies between the Si conduction band to the metal Fermi level contribute to the dark current flow. In the depletion condition, on the other hand, electrons in the metal tunnel to interface states and then they are injected to the Si conduction band. Since the interface states with an energy at the metal Fermi level have a minimum activation energy, such interface states contribute to the dark current flow but interface states with energies far below

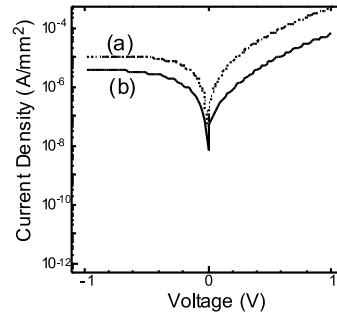


Fig. 8. The  $I - V$  curves for the  $\langle \text{Al}/2.3\text{nmSiO}_2/\text{Si}(100) \rangle$  MOS diodes: (a) with no treatment; (b) with crown-ether cyanide treatment

the metal Fermi level do not. This consideration can well explain the experimental result that the cyanide treatment decreases the dark current density in the forward bias region to a greater extent than that in the reverse bias region.

The barrier height formed between Al and n-Si is low due to a small difference in the work-functions. For measurements of leakage current characteristics of MOS diodes, the barrier height should be low (ideally no band-bending in Si at zero bias), in order to allow most of the bias voltage to be applied across the  $\text{SiO}_2$  layer. In this case, the ideality factor becomes large because most of the external bias voltage is applied across the  $\text{SiO}_2$  layer. In the case of the  $\langle \text{ITO}/\text{SiO}_2/\text{n-Si}(100) \rangle$  MOS solar cells, a high energy barrier is formed, and moreover, the  $\text{SiO}_2$  thickness is very thin, both leading to a much lower ideality factor than that for the  $\langle \text{Al}/\text{SiO}_2/\text{n-Si}(100) \rangle$  MOS diodes.

#### 4 Conclusions

Cyanide treatment which simply involves immersion of Si materials in KCN solutions can passivate defect states in a-Si and interface states at Si/ $\text{SiO}_2$  interfaces. The detailed investigation leads to the following results and conclusions.

- 1) Decreases in the photo- and dark current densities of i-a-Si layers are prevented by the crown-ether cyanide treatment under bias, and this prevention is attributed to the elimination of defect precursor states which convert to defect states by irradiation, by the reaction with  $\text{CN}^-$  ions.
- 2) The initial conversion efficiency of pin-junction a-Si solar cells increases by about 30% with the aqueous cyanide treatment and this increase is attributed to passivation of defect states in the band-gap of a-Si present before irradiation.
- 3) The energy conversion efficiency of  $\langle \text{ITO}/\text{SiO}_2/\text{single crystalline Si} \rangle$  MOS solar cells is increased by the cyanide treatment, and this increase is attributed to the passivation of Si/ $\text{SiO}_2$  interface states.

- 4) Si-CN bonds formed by the reaction of defect states with CN<sup>-</sup> ions have a high bond energy of ~4.5 eV and consequently the bonds are not ruptured by heat treatments at 800°C.
- 5) The leakage current density flowing through ultrathin SiO<sub>2</sub> layers is decreased to 1/8 up to about 1/3 by the crown-ether cyanide treatment and this decrease is attributed to the elimination of Si/SiO<sub>2</sub> interface states.

#### References

- [1] M. Isomura, N. Hata, S. Wagner: *Jpn. J. Appl. Phys.* **31** (1992) 3500
- [2] D. L. Staebler, C. R. Wronski: *Appl. Phys. Lett.* **31** (1977) 292
- [3] R. Jones, G. M. S. Lister: *Philos. Mag.* **61** (1990) 881
- [4] M. Stutzmann, W. B. Jackson, C. C. Tsai: *Phys. Rev. B* **32** (1985) 23
- [5] N. Orita, T. Matsumura, H. Katayama-Yoshida: *J. Non-Cryst. Solids* **198 – 200** (1985) 23
- [6] T. Shimizu, M. Kumeda: *J. Appl. Phys.* **35** (1996) L816
- [7] F. Irrera: *J. Appl. Phys.* **75** (1994) 1396
- [8] D. Redfield, R. H. Bube: *Phys. Rev. Lett.* **65** (1990) 464
- [9] H. Fritzsche: *Solid State Commun.* **94** (1995) 953
- [10] H. C. Card: *Solid-State Electron.* **20** (1977) 971
- [11] *The International Technology Roadmap for Semiconductors 2001*,
- [12] M. L. Reed, J. D. Plummer: *J. Appl. Phys.* **63** (1988) 5776
- [13] T. W. Hickmott: *J. Appl. Phys.* **48** (1988) 5776
- [14] S. M. Myer: *J. Appl. Phys.* **61** (1987) 5428
- [15] *CRC Handbook of Chemistry and Physics, 75th ed.*, CRC, Boca Raton: FL 1995
- [16] K. Cheng, J. Lee, J. W. Lyding: *Appl. Phys. Lett.* **77** (2000) 3388
- [17] P. J. Caplan, E. H. Poindexter, B. E. Deal, R. R. Razouk: *J. Appl. Phys.* **50** (1979) 5847
- [18] J. H. Stathis, E. Cartier: *Phys. Rev. Lett.* **72** (1994) 2745
- [19] E. H. Poindexter, P. J. Caplan: *Prog. Surf. Sci.* **14** (1983) 201
- [20] H. Kobayashi, S. Tachibana, K. Yamanaka, Y. Nakato, K. Yoneda: *J. Appl. Phys.* **81** (1997) 7630
- [21] H. Kobayashi, A. Asano, S. Asada, T. Kubota, Y. Yamashita, K. Yoneda, Y. Todokoro: *J. Appl. Phys.* **83** (1998) 2098
- [22] H. Kobayashi, A. Asano, M. Takahashi, K. Yoneda, Y. Todokoro: *Appl. Phys. Lett.* **77** (2000) 4392
- [23] E. Kanazaki, K. Yoneda, Y. Todokoro, M. Nishitani, H. Kobayashi: *Solid State Commun.* **113** (2000) 195
- [24] H. Kobayashi, Y. Kogetsu, T. Ishida, Y. Nakato: *J. Appl. Phys.* **74** (1993) 4756
- [25] T. Ishida, H. Kouno, H. Kobayashi, Y. Nakato: *J. Electrochem. Soc.* **141** (1994) 1357
- [26] M. Breiter, P. Delahay: *J. Am. Chem. Soc.* **81** (1959) 2938
- [27] E. H. Nicollian, A. Goetzberger: *Bell. Syst. Tech. J.* **46** (1967) 1055
- [28] S. M. Sze: *Physics of Semiconductor Devices, 2nd ed.*, Wiley, New York 1981
- [29] T. Sakoda, M. Matsumura, and Y. Nishioka: *Appl. Surf. Sci.* **117 –118** (1997) 241